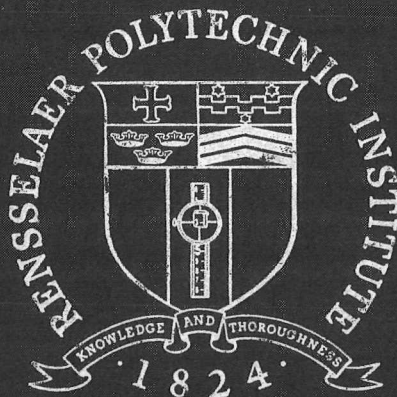


N73-10523

LASER RANGE MEASUREMENT
FOR
A SATELLITE NAVIGATION SCHEME
AND
MID-RANGE PATH SELECTION
AND
OBSTACLE AVOIDANCE

by

Gerald D. Zuraski



Rensselaer Polytechnic Institute

Troy, New York 12181

N73-10523

R.P.I. Technical Report MP-26

LASER RANGE MEASUREMENT
FOR
A SATELLITE NAVIGATION SCHEME
AND
MID-RANGE PATH SELECTION
AND
OBSTACLE AVOIDANCE

by

Gerald D. Zuraski

National Aeronautics and Space
Administration

Grant NGL 33-018-091

A project submitted to the Graduate
Faculty of Rensselaer Polytechnic Institute
in partial fulfillment of the
requirements for the degree of

MASTER OF ENGINEERING

**CASE FILE
COPY**

School of Engineering
Rensselaer Polytechnic Institute

June, 1972

TABLE OF CONTENTS

	Page
LIST OF ILLUSTRATIONS	ii
LIST OF TABLES	iii
LIST OF SYMBOLS	iv
ACKNOWLEDGEMENT	vi
ABSTRACT	vii
I. Introduction	1
II. Range Measurement for Passive Satellite Navigation	2
A. Principles of Operation	2
B. Range Errors	4
C. Power Losses	11
D. Weight Considerations	13
III. Laser Rangefinder for Mid-Range Path Selection and Obstacle Avoidance	15
A. Range Measurement Errors	15
B. Target Cross Section	23
C. Detectors	30
D. Lasers	32
E. Electronic Scanners	35
IV. Conclusions	36
REFERENCES	38

LIST OF ILLUSTRATIONS

	Page
1. Laser Rangefinder System for Passive Satellite Navigation	3
2. Range Error Due to Refraction	9
3. Optical Collector Weight	14
4. Quantization of the Time Measurement	18
5. Probability Density Functions of the Quantization Errors	19
6. Noise Error in the Received Pulse	21
7. Coordinate System for Bidirectional Reflectance	27
8. V-Groove Cavity Model for Reflection from a Rough Surface	28
9. Bidirectional Reflectance Ratio	29
10. Spectral Reflectance	31
11. Scanning System	37

LIST OF TABLES

	Page
I. Weight, Peak Transmitted Power, and Receiver Area as a Function of Transmitter Beam Divergence	16
II. Peak Transmitter Power Requirements for Various Values of Range and Target Reflectivity	25
III. Photodiode Characteristics	33
IV. Wavelength of Several Semiconductor Lasers	34

LIST OF SYMBOLS

- R = Range (m)
- T = Period of the counter clock (sec.)
- n = Number contained in the counter
- c = Speed of light (3×10^8 m/sec.)
- τ = Laser pulse width (sec.)
- Δf = Spectrum width of laser pulse shape (Hz)
- σ_R = Standard deviation of range error (m)
- $(S/N)_E$ = Signal-to-noise ratio in energy
- B = Second moment of the transmitted spectrum
- ν = Frequency of light (Hz)
- λ = Wavelength of light (m)
- f = Frequency (Hz)
- \bar{E} = Spectral density (volts/Hz^{1/2})
- t = Time (sec.)
- q = Electron charge (coul)
- η = Quantum efficiency
- h = Plank's constant (joule-sec)
- P_r = Received power (watts)
- M = Internal multiplication factor
- BW = Bandwidth (Hz)
- k = Boltzman constant = $1.38(10)^{-23}$ joule/^oK
- T_a = Temperature (^oK)
- R_{eq} = Equivalent load resistance (ohms)
- P_B = Background power (watts)
- I_d = Dark current (amps)
- ΔR_{max} = Maximum quantization error (m)
- ΔR = Range error caused by change in c
- m = Index of refraction
- H = Height (m)
- ρ = Radius of curvature (m)
- R_o = True distance (m)
- α = (μ rad) Total bending angle
- ϵ = (μ rad) Refraction angle
- Δ = Displacement on receiving plane (m)
- μ = Efficiency of optics
- ϕ_a = One-way atmospheric loss
- ϕ_T = Reflective loss at the satellite
- A_r = Receiver area (cm²)
- A_T = Target area (m²)
- ϕ_r = Returned beam divergence angle (rad.)
- ϕ_t = Transmitted beam divergence angle (rad.)
- P_t = Transmitted power (watts)

- N_{\max} = Maximum number of times the laser must be fired to search a 45° cone
- E = Energy to fire laser once (joules)
- η_L = Laser efficiency
- W = Weight (lbs)
- t_1 = Start of time interval measurement (sec.)
- t_2 = End of time interval measurement (sec.)
- t_1' = Start of quantized measurement (sec.)
- t_2' = End of quantized measurement (sec.)
- x = Error at the end of the time interval measurement (sec.)
- y = Error at the beginning of the time interval measurement (sec.)
- e = Net error (sec.)

- \bar{e} = Mean value of net error (sec.)
- σ_e^2 = Variance of net error (sec.²)
- S = Signal amplitude (volts)
- N = Noise amplitude (volts)
- m_{ave} = Average slope (volts/sec.)
- Δt = Time error due to noise (sec.)
- P_f = False alarm probability
- K = Threshold
- P_d = Probability of detection
- $(S/N)_p$ = Signal-to-noise ratio in power (watts/watt)
- S/N = Signal-to-noise ratio in amplitude (volts/volt)
- Θ = Angle between the mean surface normal and the receiver (rad.)
- r = Reflectivity
- P = Bidirectional reflectance
- g = Scale factor
- ϕ = Angle between receiver and y - z plane
- Ψ = Angle between incident beam and mean surface normal
- F = Fresnel reflectance
- \hat{n} = Complex index of refraction for normal incidence
- G = Masking and shadowing factor
- Θ_p = Projection of Θ onto the plane determined by the facet normal and the surface normal
- Ψ_p = Projection of Ψ onto the plane determined by the facet normal and the surface normal
- C = A constant
- γ = Angle between facet normal and surface normal
- l = Width of one side of a V-groove cavity (cm)
- m' = Part of V-groove cavity masked (cm)

ACKNOWLEDGEMENT

The author wishes to express his gratitude to Prof. C. N. Shen for his advice and assistance as Faculty Advisor during the preparation of this work.

ABSTRACT

A laser rangefinder may be used to perform two functions on board an autonomous Martian roving vehicle. These two functions are (1) navigation by means of a passive satellite and (2) mid-range path selection and obstacle avoidance. The feasibility of using a laser to make the necessary range measurements is explored in detail and a preliminary design is presented. The two uses of the rangefinder dictate widely different operating parameters making it impossible to use the same system for both functions.

I. INTRODUCTION

A laser rangefinder may be used to perform two functions on board the Martian roving vehicle. These two functions are (1) navigation by means of a passive satellite and (2) mid-range path selection and obstacle avoidance. It will be shown that the laser used for navigation would not be used for obstacle avoidance because of the great differences in operating power levels and repetition rates.

The satellite navigation scheme for the Martian rover requires the measurement of the distance between the rover and a passive satellite in order to locate the rover in a Mars reference frame.^[1] The distance to be measured is of the order of several thousand kilometers and must be measured to within an accuracy of several meters. A laser rangefinder combined with a retroreflecting surface on the satellite will be shown to meet the requirements of the navigation scheme. Of primary concern are the weight and power requirements of the system. An attempt has been made to include as many factors as possible in the calculation of the power requirements for a given accuracy while at the same time using as simple a system as possible for reliability.

Instrumentation for a mid-range path selection and obstacle avoidance system has also been investigated. A laser rangefinder is to be used to sense terrain three to thirty meters ahead of the Mars roving vehicle. The major components of the system are (1) the laser, (2) the photodetector, and (3) a scanning system. The parameters of these components are dictated by the terrain reflectivity, the range to be covered, and the scan rate. The scan rate is determined by the particular path selection algorithm to be used, some algorithms requiring more data than others. The 'ideal' system would minimize

power and weight, while adequately defining terrain to ensure vehicle safety. A range accuracy of five centimeters or less is thought to be necessary in order to adequately define terrain slopes three to thirty meters ahead of the vehicle.

This report is divided into two parts. The first part is a discussion of the satellite navigation system. The second part deals with the path selection and obstacle avoidance system.

PART II PASSIVE SATELLITE NAVIGATION SYSTEM

A. Principles of Operation.

The laser rangefinder operates in a manner similar to that of a conventional radar. A block diagram of the essential elements of the system is shown in Figure 1. The measurement procedure is initiated by a trigger pulse from the on-board computer. The trigger pulse causes the laser to fire a single short pulse of light. A small photodetector mounted on the laser senses the leading edge of the light pulse and starts the counter. The trigger pulse from the on-board computer is not used to start the counter because there is a time delay involved in firing the laser. The light pulse from the laser travels to the satellite, is reflected and returns to a light receiver. The satellite is equipped with a retroreflecting surface so that the light incident upon the satellite will be reflected back to the rover, independent of the orientation of the satellite. The light receiver collects the reflected light and focuses it on a photodetector. The output of this photodetector stops the counter. The counter now contains a number

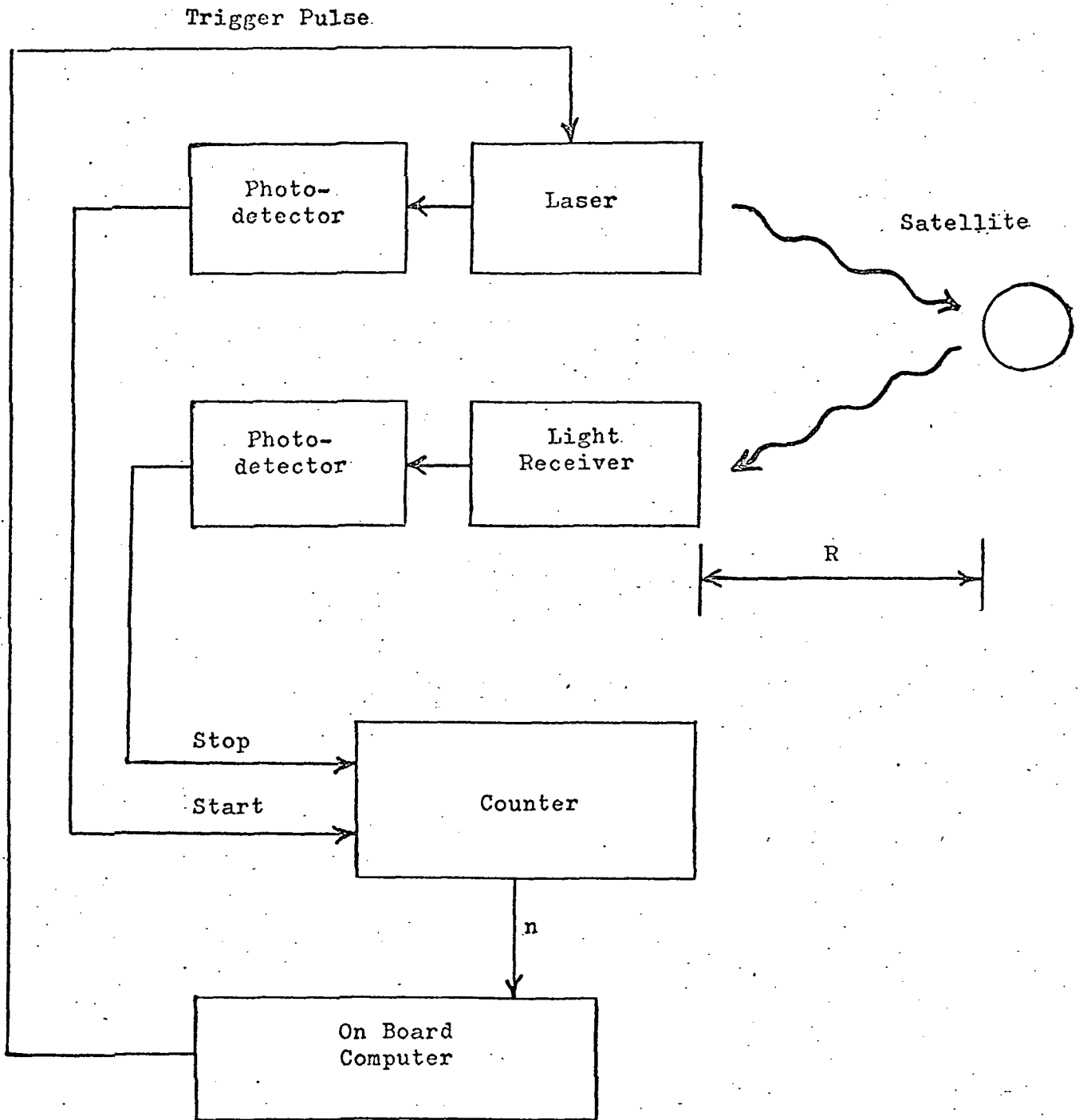


Figure 1

LASER RANGEFINDER SYSTEM FOR PASSIVE SATELLITE NAVIGATION

which is proportional to the distance between the rangefinder and the satellite. The on-board computer reads out this number and computes the one-way range from the following simple equation:

$$R = \frac{cnT}{2}$$

where R = Distance to the satellite (km)

T = Period of the counter clock (sec.)

n = Number contained in the counter

c = Speed of light (3×10^5 km/sec.)

For $T = 10^{-9}$ seconds and $n = 1.33(10)^7$, the range is given by:

$$R = \frac{(3)(10)^5(1.33)(10)^7(10)^{-9}}{2} = 2000 \text{ kilometers}$$

Note that the counter must be eight decades long in order to record n. It may be possible to use a shorter counter if the range between the satellite and the rover always falls within a small interval. In this case, the most significant 'bits' of the counter will always be the same, so that part of the counter is not needed.

B. Range Error

The range error is primarily a function of the counter clock period, the pulse width of the laser, the signal-to-noise ratio at the receiver, variation in the speed of light passing through atmosphere, and refraction. One way to analyze the range error due to the finite pulse width of the laser and the signal-to-noise ratio is given here. The laser pulse width is τ and has a band limited spectrum of width Δf . Assume the noise is gaussian and occupies the same frequency band Δf . It can now be shown [2] that the range error is zero mean gaussian with

standard deviation given by:

$$R = \frac{c}{4 \pi B(S/N)_E^{1/2}} \quad (1)$$

where $(S/N)_E$ = Signal-to-noise ratio in energy

B = Second moment of the transmitted spectrum (Hz)

Some care must be exercised in calculating the signal-to-noise ratio $(S/N)_E$ and the second moment B . The transmitted signal can be viewed as a carrier frequency ν modulated by a time signal which has the same waveform as the pulse shape of the laser output. The carrier frequency is just the frequency of the laser light and is given by:

$$\nu = \frac{c}{\lambda}$$

where λ = wavelength of the light output of the laser

For example, a ruby laser has $\lambda = 6945 \text{ \AA} = .6945 \mu\text{m} = 6.945(10)^{-7}\text{m}$

then

$$\nu = \frac{3(10)^8}{6.945(10)^{-7}} = 4.32(10)^{14} \text{ Hz}$$

The second moment B is given by:

$$B = \left[\frac{\int_{\Delta f} (f - \nu)^2 |\Phi(f)|^2 df}{\int_{\Delta f} |\Phi(f)|^2 df} \right]^{1/2}$$

where $\Phi(f)$ = Transmitted spectrum (volts/Hz^{1/2})

As an example, consider the case where the laser pulse envelope can be approximated by $\frac{\sin 2 \pi t / \tau}{2 \pi t / \tau}$, where t is time. The corresponding

spectrum is found by taking the Fourier transform and is rectangular

of width $\Delta f = 2/\tau$. For $\tau = 10$ nsec, $\Delta f = 2(10)^8$ Hz. Since the spectrum is rectangular, $B = \Delta f/2\sqrt{3} = 5.77(10)^7$ Hz. The signal-to-noise ratio in energy at the input to the receiver is equal to the signal-to-noise ratio in power at the output of an ideal receiver (correlation receiver). If a non-ideal receiver is used the signal-to-noise ratio at the output will be less than that at the input. Therefore Equation (1) gives an upper bound on the range accuracy to be expected. Continuing the example, for $(S/N)_E = 10$, the r.m.s. range error would be 13 cm. If the transmitted spectrum is approximately bell shaped, B is equal to one-half the 3 dB width of the spectrum. It can be concluded that for $(S/N)_E = 10$ and $\tau = 10$ nsec, the range error will be less than one meter..

The signal-to-noise ratio can be calculated if the type of detector, received power, and background radiation are known. The general equation for the signal-to-noise ratio of a photomultiplier tube is [3]:

$$S/N = \frac{\left[\frac{q\eta}{h\nu} \right]^2 M^2}{BW \left[\frac{2kT_a}{R_{eq}} + 4qM^2 \left(\frac{q\eta P_r}{h\nu} + \frac{q\eta P_B}{h\nu} + I_d \right) \right]} \quad (2)$$

where q = Electron charge = $1.6(10)^{-19}$ coul.

η = Quantum efficiency of photomultiplier

h = Plank's constant = $6.63(10)^{-34}$ joule-sec.

P_r = Received Power (watts)

M = Internal signal multiplication factor

BW = Bandwidth (Hz)

k = Boltzman constant = $1.38(10)^{-23}$ joule/ $^{\circ}$ K

T_a = Temperature ($^{\circ}$ K)

R_{eq} = Equivalent load resistance (ohms)

P_B = Background power falling on the detector (watts)

I_d = Dark current (amps)

A similar expression exists for photodiodes and will be given later.

The first term in the denominator of Equation (2) represents thermal noise and is generally insignificant in a well designed photomultiplier. The last three terms represent shot noise from the received signal, the background signal, and the dark current, respectively. The background signal can be minimized by use of a narrowband light filter and by limiting the field of view of the receiver. For $BW = (10)^7$ Hz, $\eta = 0.02$, $M = 4.7(10)^6$, $\nu = 4.32(10)^{14}$ Hz, $I_d = 8(10)^{-14}$ amp., $P_r = 0.6(10)^{-8}$ watts, negligible background radiation, and shot noise limited operation, the signal-to-noise ratio is 10. This is typical of an S-20 photomultiplier [3].

The quantization error due to the digital counter can be expressed as: $\Delta R_{max} = cT/2$ where ΔR_{max} = the maximum range error due to quantization. Since nanosecond counters are available, this error is small ($\Delta R_{max} = 15$ cm for $T = 1$ nsec) and will not be considered further.

The velocity of light, c , varies with the properties of the medium. For example, the velocity of light in vacuum and the velocity of light in air at STP agree only to about one part in a thousand [4]. The velocity of light in a vacuum is known to one part in $(10)^6$. The velocity of light in the Martian atmosphere can be approximated if the atmospheric composition can be determined and the range error can then be estimated as a function of the path length through the atmosphere. If it is assumed that the average path length through the atmosphere is 5 km and that c is changed by one part in $(10)^4$ over this entire length

the resulting range error can be derived as follows:

$$R = \frac{cT}{2} \quad (3)$$

$$R + \Delta R = \frac{(c + \Delta c)t}{2} \quad (4)$$

Subtracting Equation (3) from Equation (4) gives:

$$\Delta R = \frac{\Delta c t}{2} \quad (5)$$

Rearranging Equation (3).

$$\frac{t}{2} = \frac{R}{c}$$

and substituting into Equation (5) gives

$$\Delta R = \frac{\Delta c}{c} R$$

Therefore,

$$\Delta R = (10)^{-4} (5) (10)^3 = 0.5 \text{ m}$$

From this example, it can be concluded that range errors due to changes in c caused by atmosphere are less than or at worst of the order of one meter.

The range error due to refraction can be upper bounded by using earth data. This error arises from bending of the laser beam caused by changes in the index of refraction m . The index of refraction varies approximately exponentially with height and is assumed to be constant at a given altitude. Under these assumptions, there would be no bending of the laser beam if it is pointed straight up. However, as the beam is moved toward the horizon, bending does occur. The error due to refraction for a horizontal measurement is illustrated in Figure 2. It can be shown [5] that:

$$\rho = \frac{-1}{\left(\frac{dm}{dh}\right)}$$

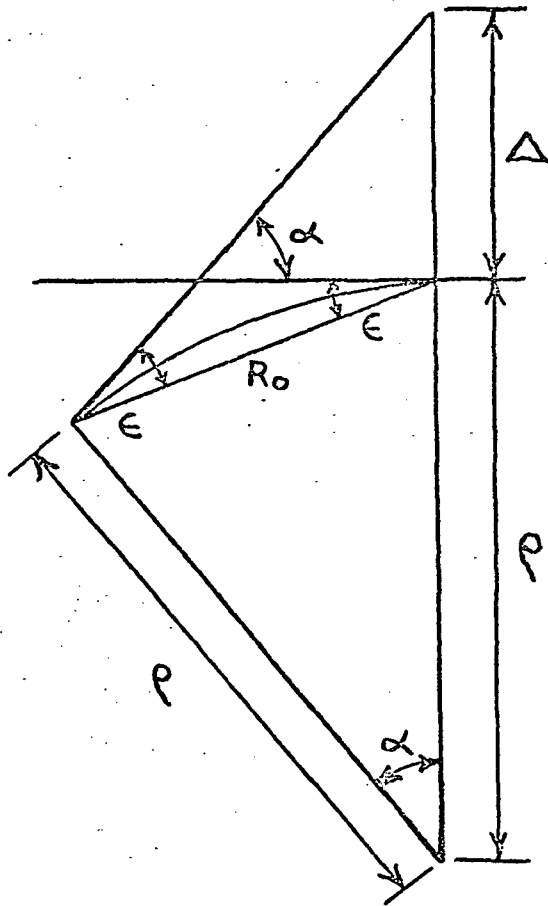


Figure 2

RANGE ERROR DUE TO REFRACTION

where ρ = Radius of curvature

m = Refractive index

H = Height

Also, $2 \epsilon = \alpha$ and $\epsilon = -\frac{R_0}{2} \frac{dm}{dH}$

where R_0 = True distance (m)

ϵ = Refraction angle (rad)

α = Total bending angle (rad)

The displacement of the spot on the receiving plane is:

$$\Delta = R_0 \epsilon$$

ϵ has been measured to be as large as 40μ rad/km on earth, and Δ is typically 1.35 m for a 10 km measurement distance on earth. The measured path length is given by:

$$R = \rho \alpha$$

The true path length is:

$$R_0 = 2\rho \sin\alpha/2$$

The error is then

$$\Delta R = R - R_0 = \rho (\alpha - 2\sin\alpha/2)$$

Since α is a small angle,

$$\Delta R \left[\alpha - 2\left(\frac{\alpha}{2} - \frac{\alpha^3}{48}\right) \right] = \rho \frac{\alpha^3}{24}$$

or

$$\Delta R \approx \frac{R\alpha^2}{24} = \frac{R\epsilon^2}{6}$$

If we assume a worst case refraction angle of 400μ rad and a range of 100 km, the error is:

$$\Delta R = \frac{(10)^5(400)^2(10)^{-12}}{6} = 0.26 \text{ cm}$$

Thus, we see that this error is extremely small and need not be considered further.

C. Power Losses

The power output required of the laser can be determined from the minimum received power necessary to achieve the required signal-to-noise ratio and the power losses along the transmission path. The transmitted power and received power are related by [1]:

$$P_r = \left[\frac{\mu \phi_a^2 \phi_T A_r A_T}{\pi^2 \phi_r^2 \phi_t^2 R^4} \right] P_t \quad (6)$$

where P_r = Power received (watts)

μ = Efficiency of the optics

ϕ_a = One-way atmospheric loss

ϕ_T = Reflective loss at the satellite

A_r = Receiver area (km²)

A_T = Target area (km²)

ϕ_r = Returned beam divergence angle (rad)

ϕ_t = Transmitted beam divergence angle (rad)

P_t = Transmitted power (watts)

R = One-way range (km)

For $\mu = .9$, $\phi_a = .9$, $A_r = 200 \text{ cm}^2$, $\phi_t = 1.7(10)^{-2} \text{ rad.}$, $\phi_r = 0.6(10)^{-4} \text{ rad.}$, $\phi_T A_T = 2 \text{ m}^2$, and $R = 2000 \text{ km}$:

$$P_r = 1.97(10)^{-16} P_t$$

These numbers are typical for measuring the distance to the satellite.

From a previous example, $P_r = .6(10)^{-8}$ watts for a signal-to-noise ratio of 10. The required peak transmitter power is then:

$$P_t = \frac{.6(10)^{-8}}{1.97(10)^{-16}} = 3.0(10)^7 \text{ watts}$$

An estimate of the average power requirements of the laser can be

made based upon the peak transmitted power P_t , the pulse width τ , the transmitted beam divergence ϕ_t , the search area, the efficiency of the laser, and the number of measurements to be made. From the previous example, $P_t = 3(10)^7$ watts for $\phi_t = 1.7(10)^{-2}$ rad. If we wish to search over a 45° solid cone, the maximum number of times the laser must be fired is approximately:

$$N_{\max} = \frac{\tan^2(45^\circ/2)}{\tan^2 \phi_t} = \frac{\tan^2 0.392}{\tan^2 0.017} = 590$$

Three range measurements are required to determine the position of the rover relative to the satellite. These three measurements are made within a small time interval (one second) and therefore the entire 45° cone need not be searched for the second and third measurements. The average number of laser firings will be taken to be 300. If we wish to locate the rover once per day (24 hrs.), the total expected number of firings would be about 300 per day. The energy required to fire the laser once is given by:

$$E = \frac{P_t \tau}{\eta_L}$$

where E = Energy input (joules)

η_L = Laser efficiency

P_t = Peak power (watts)

τ = Pulse width (sec.)

For $\tau = 10$ nsec., $P_t = 3(10)^7$ watts, and $\eta_L = .005$,

$$E = \frac{3(10)^7(10)^{-8}}{.005} = 60 \text{ joules}$$

The total energy required per day would then be $300 \times 60 = 18000$ joules.

The average power of the laser is then $18000/(3600)(24) = 0.208$ watts.

From a practical standpoint, it would be desirable to make the measurements

over as short a time as possible. Thus if we allow 15 watts continuous operating power, we could make our measurements in about 20 minutes. These measurements could be done during the Martian night, thereby reducing the background radiation entering the detector and also not interfering with roving activities during the day.

D. Weight Considerations

The two largest components of the rangefinding system which are on board the roving vehicle are the optical collector and the energy discharge capacitors. A graph of weight vs surface accuracy^[5] for several size optical collectors is shown in Figure 3. The penalty for a large blur circle is a wider field of view which results in greater background noise. It should be noted that a field stop will not correct this. If we assume a blur circle of 100 μ rad. the weight of the optical collector is about 8 lbs/ft² = 86 lbs/m². Pulse discharge capacitors suitable for use with lasers are available with energy storage capabilities of up to 125 joules/lb.^[6]

For $\eta_L = 0.005$ and $\tau = 10$ nsec, the peak transmitter power per pound of capacitor is:

$$P_t/lb = \frac{(125)(.005)}{(10)^{-8}} = 6.25(10)^7 \text{ watts/lb}$$

Rearranging Equation 6 and using previously stated parameter values gives:

$$P_t A_r = 2.08(10)^9 \phi_t^2 \quad (7)$$

The total weight of the system can now be written as:

$$W = 86 A_r + 1.6(10)^{-8} P_t + 5 \quad (8)$$

Taking the derivative with respect to A_r and setting equal to zero gives:

$$\frac{\partial W}{\partial A_r} = 0 = 86 + 33.2(-2) \frac{\phi_t^2}{A_r^2}$$

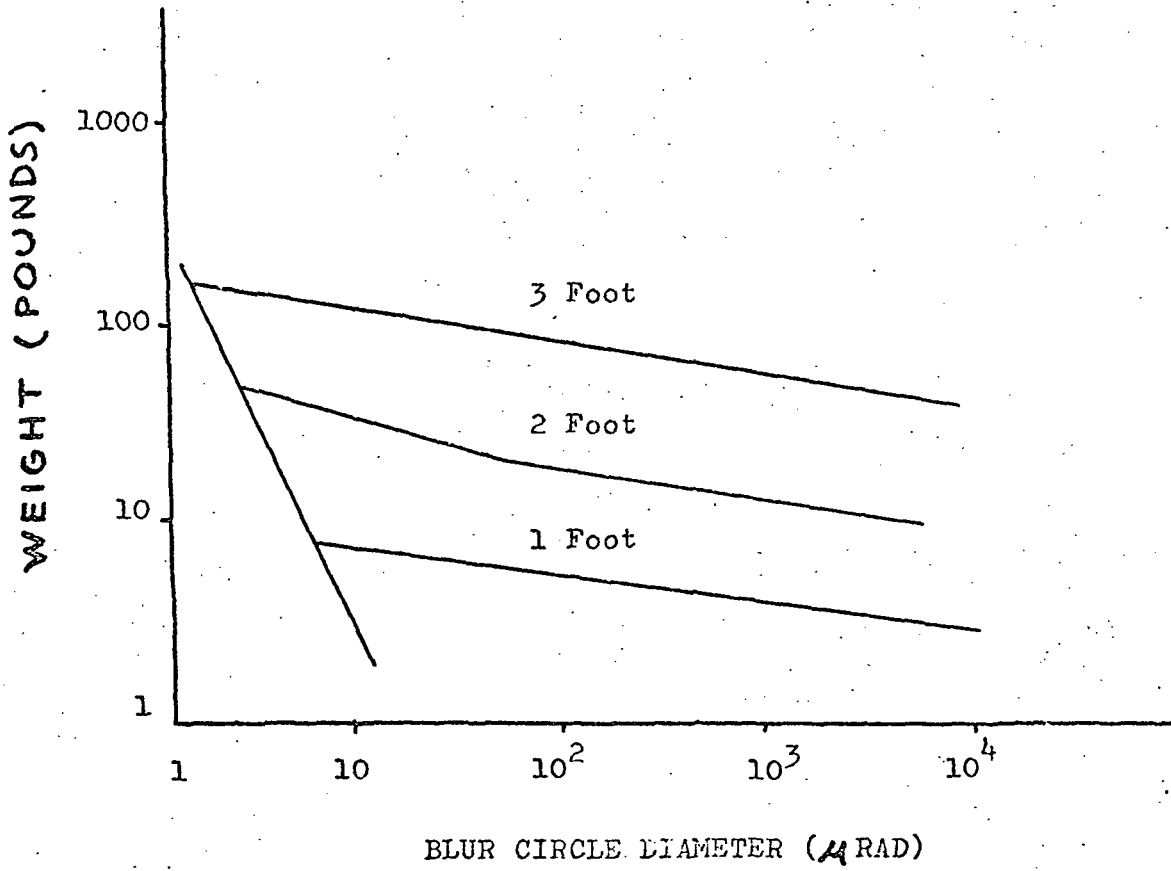


Figure 3

OPTICAL COLLECTOR WEIGHT

$$A_r = .88 \phi_t$$

$$P_t = 2.36(10)^9 \phi_t$$

$$W = 113.5 \phi_t + 5$$

Table I shows how these parameters vary as a function of the transmitted beam divergence angle. The weight of the rangefinding system is seen to be proportional to the transmitted beam divergence. The weight can be reduced by requiring a smaller beam divergence. However, for a smaller beam divergence, greater accuracy in the pointing system used to aim the laser is required. Also, for angles less than 1° , not much improvement in weight can be expected.

PART III LASER RANGEFINDER FOR MID-RANGE PATH SELECTION AND OBSTACLE AVOIDANCE

A. Range Measurement Errors

The range error is of considerable importance in evaluating the performance of path selection and obstacle avoidance schemes. Various schemes have been proposed which use combinations of angle and range measurements or range measurements alone. The final choice of a particular scheme will depend heavily upon the range accuracies that can be achieved. What follows is a detailed discussion of the range error.

The range is determined by transmitting a pulse of laser light to the Martian surface and measuring the light reflected back to the vehicle. Two photodetectors are employed, one senses the light emitted from the laser and the other senses the light reflected from the surface. The signal outputs of the two detectors are used to control the operation

ϕ_t (Degrees)	W (lbs)	P_t (Mw)	A_r (cm ²)
.05	5.1	2.05	7.65
.5	6.0	20.5	76.5
1.0	7.0	41.0	153
2.0	9.0	82.5	308
5	14.9	205	765
10	24.7	410	1530

TABLE I WEIGHT, PEAK TRANSMITTED POWER AND RECEIVER AREA
AS A FUNCTION OF TRANSMITTER BEAM DIVERGENCE

of a time interval meter. The errors involved in the measurement of the time interval arise from two distinct sources, noise and quantization.

The quantization process is shown in Figure 4. The time interval meter consists of three basic elements, (1) a square wave oscillator or 'clock', (2) a counter, and (3) a gating circuit. The error involved with the generation of the triggering waveform will be considered later. The triggering waveform initiates and stops the count. The true time interval (to within the accuracy of the triggering waveform) is shown in Figure 4 b and is given by:

$$t = t_2 - t_1$$

The recorded time interval (Fig. 4 c) is given by:

$$nT = t_2' - t_1'$$

Two errors occur for each measurement, one at the beginning of the count cycle and one at the end of the count cycle. The net error is the difference between these two errors:

$$e = t - nT = (t_2 - t_2') - (t_1 - t_1')$$

If we denote $t_1 - t_1'$ by y and $t_2 - t_2'$ by x (Figure 4 d), the net error is:

$$e = x - y$$

x and y can be considered as independent random variables since they arise from physically independent sources. Also, for $n \gg 1$, x and y will have uniform probability densities over the interval 0 to T . The probability density of the total quantization error can be found by convolving the density functions of x and y since x and y are independent. Figure 5 shows the density functions of x , y , and e . The mean net error e is seen to be zero by inspection of Figure 5 c. The variance of the

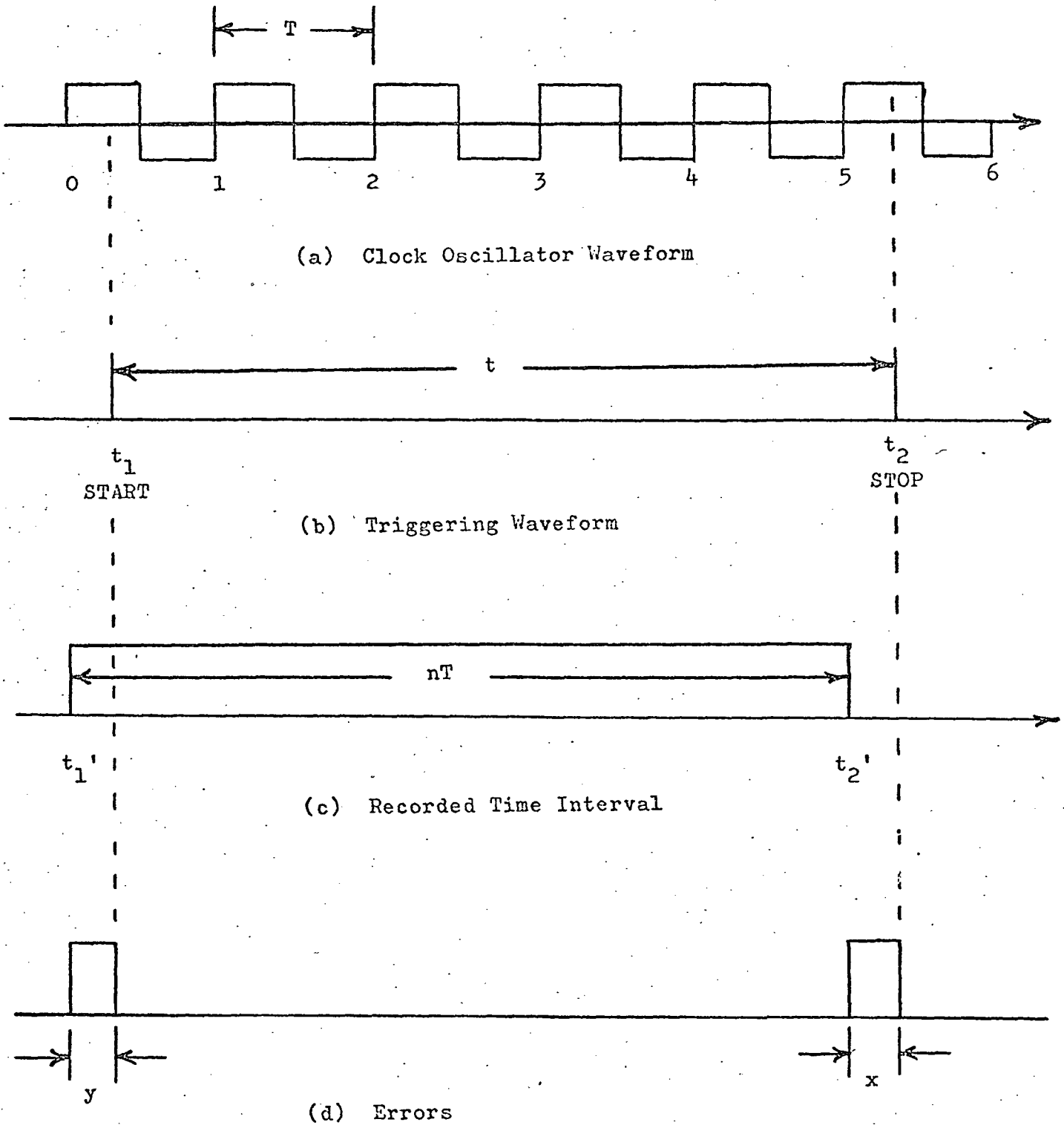
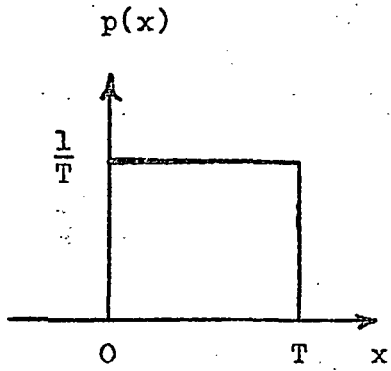
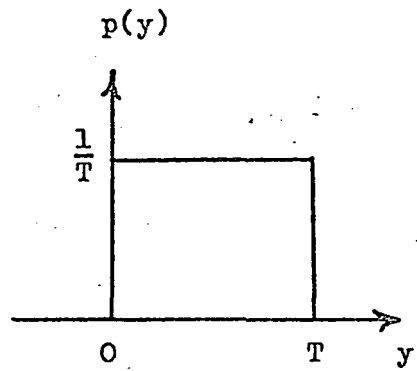


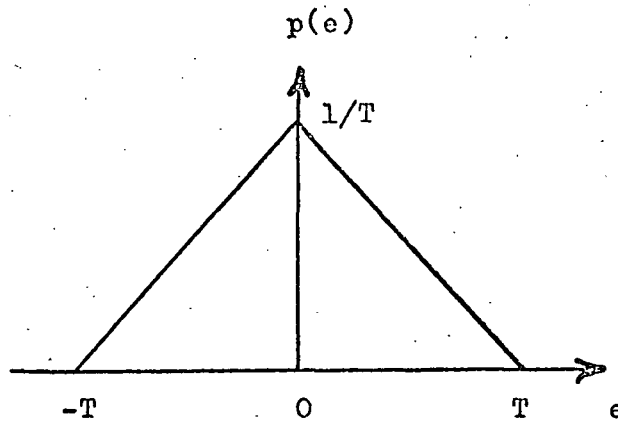
Figure 4
QUANTIZATION OF THE TIME MEASUREMENT



(a) Probability Density of x



(b) Probability Density of y



(c) Probability Density of the Net Error

Figure 5

PROBABILITY DENSITIES OF QUANTIZATION ERRORS

net error can be found as follows:

$$\sigma_e^2 = \int_{-T}^T e^2 p(e) de$$

$$\sigma_e^2 = \int_{-T}^0 e^2 \left(\frac{1}{T^2} e + \frac{1}{T} \right) de + \int_0^T e^2 \left(-\frac{1}{T^2} e + \frac{1}{T} \right) de$$

$$\sigma_e^2 = \frac{T^2}{6}$$

The standard deviation of the range error is related to the time error by:

$$\sigma_R = \frac{c \sigma_e}{2}$$

$$\sigma_R = \frac{cT}{2\sqrt{6}}$$

As an example, the standard deviation in range for a $\frac{1}{4}$ nanosecond clock period is given by:

$$\sigma_R = \frac{3(10)^8 (.25)(10)^{-9}}{2\sqrt{6}} = 1.5 \text{ cm}$$

Note also that the maximum time error is $\pm T$. For a $\frac{1}{4}$ nanosecond clock period, this corresponds to a maximum range error of ± 3.75 cm.

The accuracy of the triggering waveform has been estimated for one particular method of thresholding and will be shown to be related to the signal-to-noise ratio. The error involved in generating the start pulse at t_1 can be assumed to be negligible compared to the error involved in generating the stop pulse at t_2 since the signal-to-noise ratio will generally be much greater at t_1 than at t_2 . An upper bound on the error can be derived in terms of the average slope of the transmitted pulse and the signal-to-noise ratio. The received pulse is shown in Figure 6.

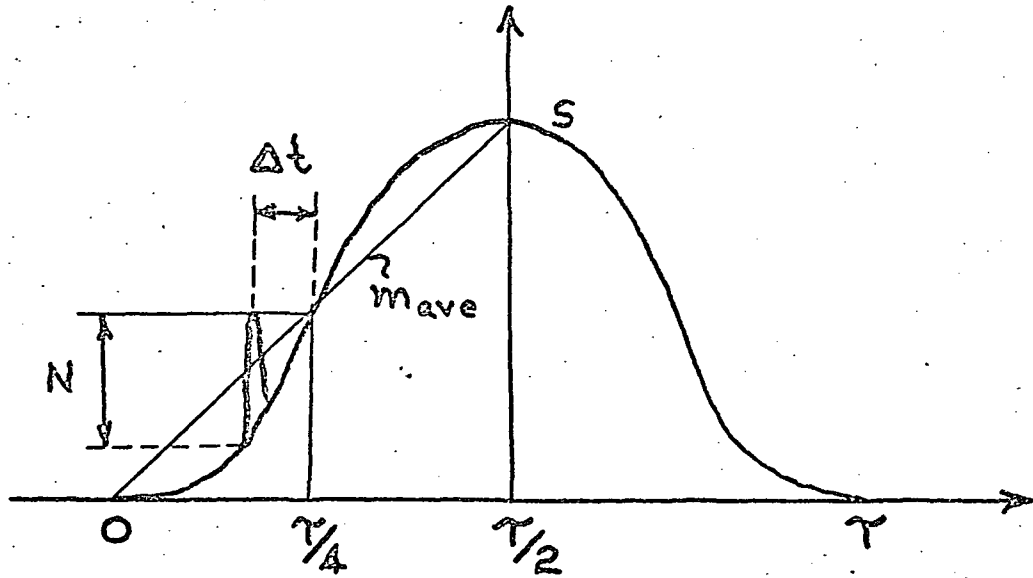


Figure 6

NOISE ERROR IN THE RECEIVED PULSE

The average slope of the noiseless signal is given by:

$$m_{ave} = \frac{2S}{\tau} \quad (9)$$

where S = Maximum amplitude of the signal (volts)

τ = Signal duration (sec.)

m_{ave} = Average slope (volts/sec.)

The pulse shape is assumed to be symmetric. If no noise is present, the thresholding device will generate a triggering pulse when the signal reaches one half of its maximum value or any other preset percentage of its maximum value. The same procedure is used to generate the start and stop triggering pulses. When there is no noise present, the only error will be the quantization error of the counter. When noise is present, it will cause an error in the generation of the stop pulse. If we denote this error by Δt , from Figure 6 the magnitude of the error is:

$$|\Delta t| \leq \frac{N}{m_{ave}} \quad (10)$$

where N = Noise amplitude (volts)

m_{ave} = Average slope (volts/sec.)

Substituting Equation 9 into Equation 10 gives:

$$|\Delta t| \leq \frac{\tau}{2(S/N)}$$

From this equation we can draw two conclusions. First, it is desirable to have as narrow a pulse width as possible, and second, the signal-to-noise ratio should be as high as possible. The range error associated with a pulse width of 10 nanoseconds and a signal-to-noise ratio of 20 is 3.75 cm maximum. It should also be noted that the timing error is minimized if the threshold point is placed at the point of steepest slope of the transmitted signal.

Associated with the signal-to-noise ratio are the detection probability and the probability of false alarm. These considerations arise when trying to decide when there is a signal peak or a noise peak. If a threshold is set at K standard deviations of the noise, the probability of false alarm P_f is [2]

$$P_f = \frac{1}{\sqrt{2\pi}} \int_K^{\infty} \exp(-v^2/2) dv$$

For $K = 3.1$, $P_f = (10)^{-3}$.

Once the false alarm probability has been given and the threshold K calculated, the signal-to-noise ratio for a given detection probability can be calculated from:

$$P_d = \frac{1}{\sqrt{2\pi}} \int_{K-S/N}^{\infty} \exp(-v^2/2) dv$$

where S/N = Signal-to-noise ratio in volts/volt

Note that $(S/N)^2 = (S/N)_p$ and that $(S/N)_E = (S/N)_p$ for an ideal receiver (matched filter). As an example, for $P_f = (10)^{-3}$, $K = 3.1$, and $(S/N)_p = 10$, $P_d = 0.5$. For $(S/N)_p = 25$, $P_d = 0.98$.

The signal-to-noise ratio for the rangefinder may be dictated by either error considerations or by false alarm rates and detection probabilities depending on which requirement is greater.

B. Target Cross Section

The power requirements of the laser are highly dependent upon the reflectivity of the terrain. A rough estimate of the peak transmitter power can be made by assuming the terrain to be an ideal diffuse surface (Lambert model). Snow is an example of such a surface. If the receiver

field of view is greater than the target area, the transmitted power can be expressed as:

$$P_t = \frac{2\pi R^2}{A_r \cos \theta} P_r$$

where P_t = Transmitted power (watts)

P_r = Received power (watts)

A_r = Receiver area (m^2)

R = One-way range (m)

θ = Angle between the mean surface normal and the receiver (rad.)

If absorption of light by the surface is taken into account this equation becomes:

$$P_t = \frac{2\pi R^2}{r A_r \cos \theta} P_r$$

where r = Target reflectivity

This equation was evaluated at several points to illustrate the magnitude of the different parameters. The results shown in Table II are for $A_r = 1 \text{ cm}^2$, $P_r = (10)^{-8}$ watts, and $\theta = 0$. The $P_t = (10)^{-8}$ watts corresponds to a signal-to-noise ratio of about 10.^[3] Note that more power is required than is shown in the table if the receiver is not perpendicular to the surface.

Experimental evidence^[7] has shown that the Lambert model is approached with increasing surface roughness only when the incident light arrives in a near-normal direction. Since the measurement schemes considered for use on the rover require the incident beam to arrive at shallow angles, a better model is needed. Such a model has been developed by Torrance and Sparrow.^[7] The major features of the model are (1) small random mirror-like facets, (2) multiple reflection, (3) internal scattering, (4) shadowing, and (5) masking. The model generally applies when the

Target Reflectivity	Range		
	R = 7 m	R = 14 m	R = 28 m
.1%	30 w	120 w	480 w
1%	3 w	12 w	48 w
10%	.3 w	1.2 w	4.8 w

TABLE II PEAK TRANSMITTER POWER REQUIREMENTS FOR VARIOUS
VALUES OF RANGE AND TARGET REFLECTIVITY

root-mean-square surface roughness is greater than the wavelength of the light used.

The reflectance distribution of a rough surface can be specified in terms of a normalized bidirectional reflectance [7]:

$$\frac{P(\Psi; \Theta, \Phi)}{P(\Psi; \Psi, 0^\circ)} = \frac{gF(\Psi, \hat{n}) [G(\Psi_p, \Theta_p) / \cos \Theta] \exp(-C^2 \gamma^2) + \cos \Psi}{g [F(\Psi, \hat{n}) / \cos \Psi] + \cos \Psi} \quad (11)$$

The angles Ψ , Θ , and Φ are shown in Figure 7. g is a scale factor which determines the ratio of specular reflection to diffuse reflection. The Fresnel reflectance $F(\Psi, \hat{n})$ is a strong function of Ψ for $60^\circ < \Psi < 90^\circ$, which is the range of angles that must be used in the rangefinding system. As an example, the Fresnel reflectance for magnesium oxide varies from .1 to 1 over the range of Ψ cited. The Fresnel reflectance also varies widely with material. The shape of the Fresnel curves differ markedly for metals and nonmetals.

The geometrical attenuation factor $G(\Psi_p, \Theta_p)$ takes into account the geometry of a rough surface. A V-groove model is used to represent a surface facet. One possible orientation of the V-groove model is shown in Figure 8. The constant C and the angle γ define the distribution of facet slopes about the mean surface plane. Typical curves for the bidirectional reflectance ratio are shown in Figure 9. The dashed line represents the Lambert model. Note that peaks in the distribution occur at angles greater than the specular angle. These off-specular peaks are caused by the factor $G/\cos \Theta$ in Equation 11. It should also be noted that $G/\cos \Theta$ is strictly geometrical in nature, and hence, all materials will exhibit some degree of off-specular peaking.

Since the actual magnitude of the bidirectional reflectance ratio is

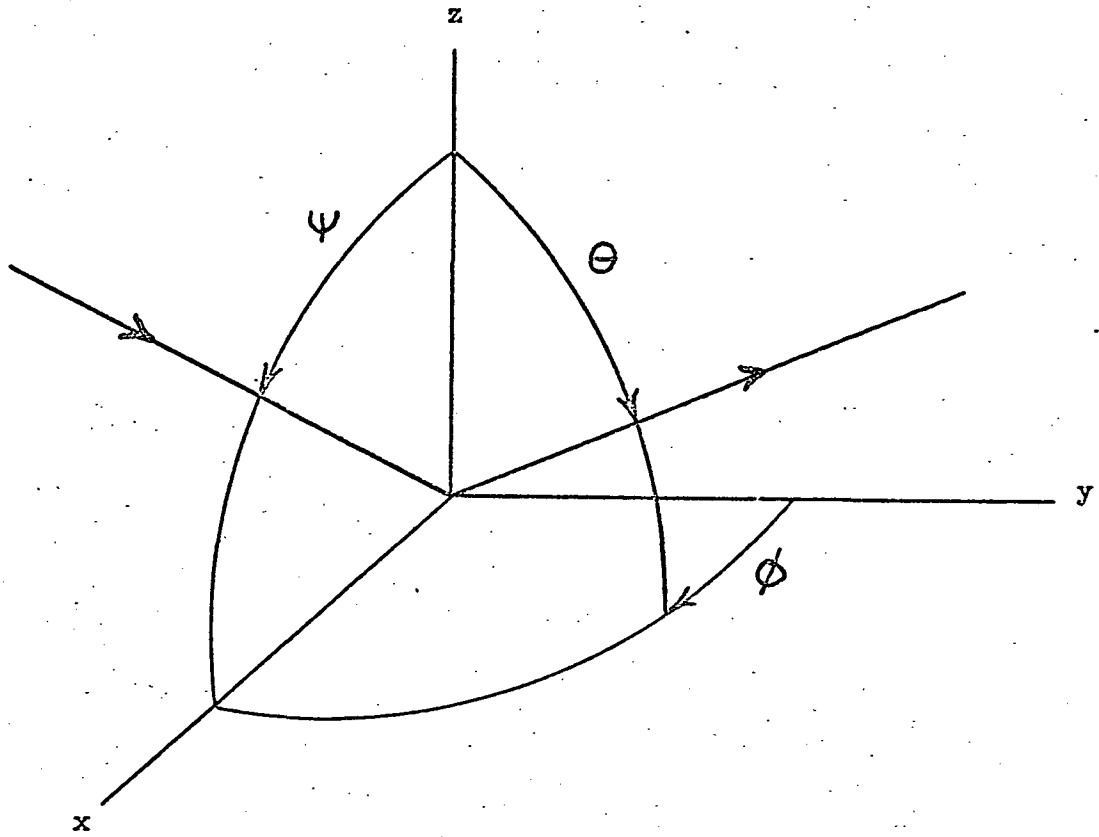
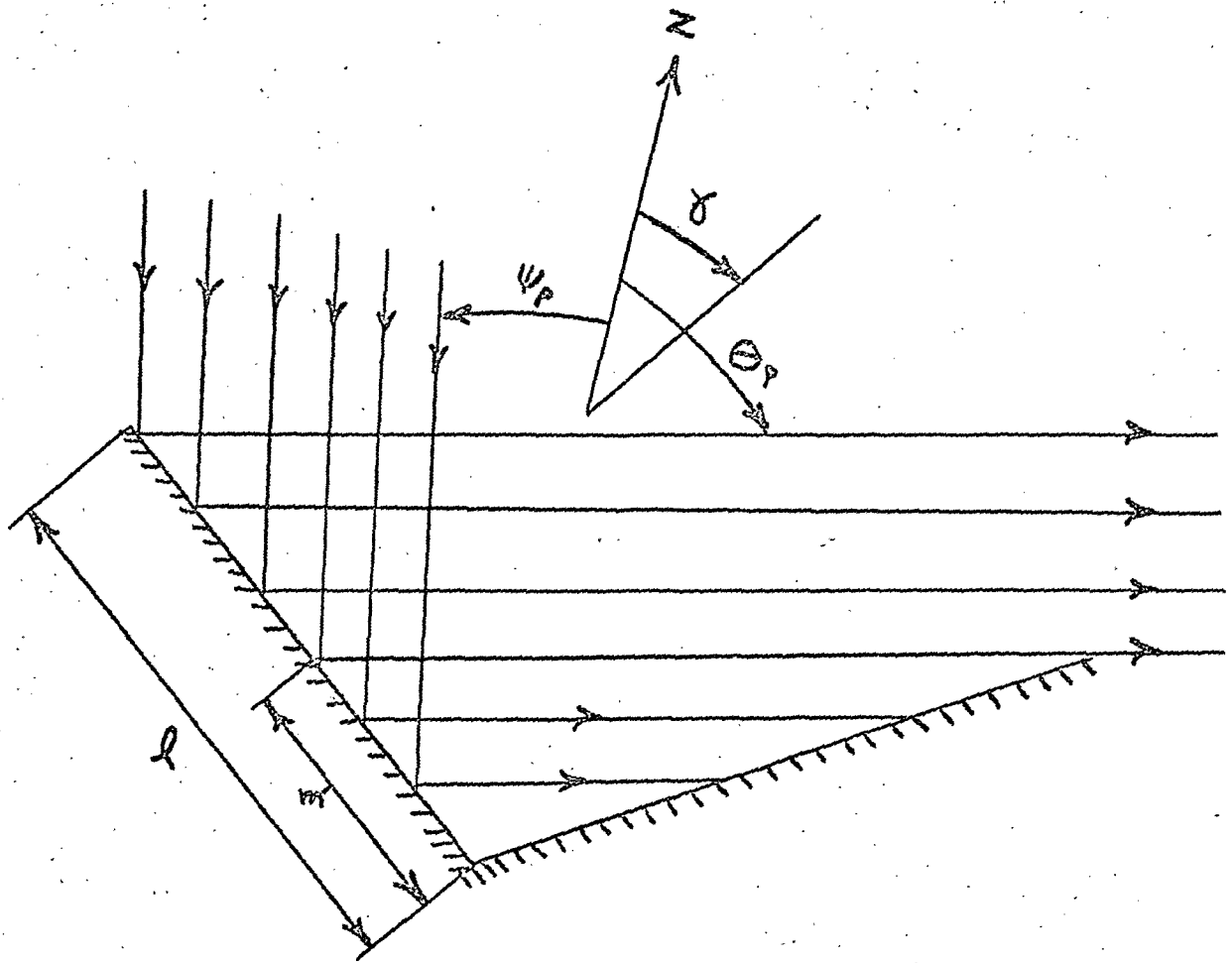


Figure 7

COORDINATE SYSTEM FOR BIDIRECTIONAL REFLECTANCE



$$G(\psi_p, \theta_p) = 1 - (m'/l)$$

Figure 8

V-GROOVE CAVITY MODEL FOR REFLECTION FROM A ROUGH SURFACE

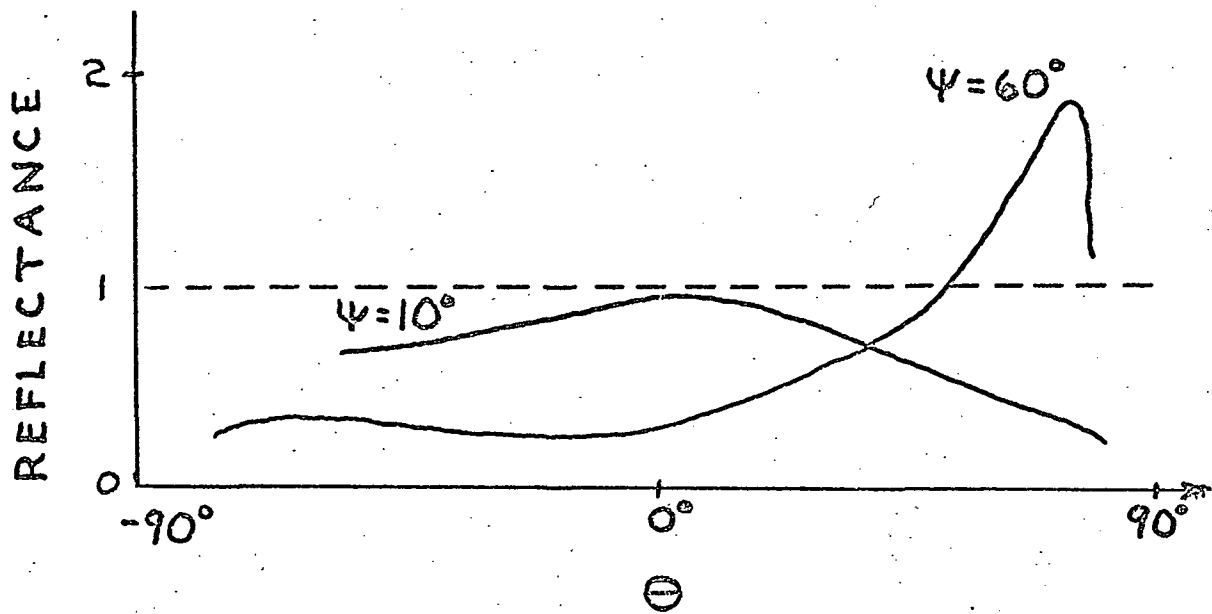


Figure 9

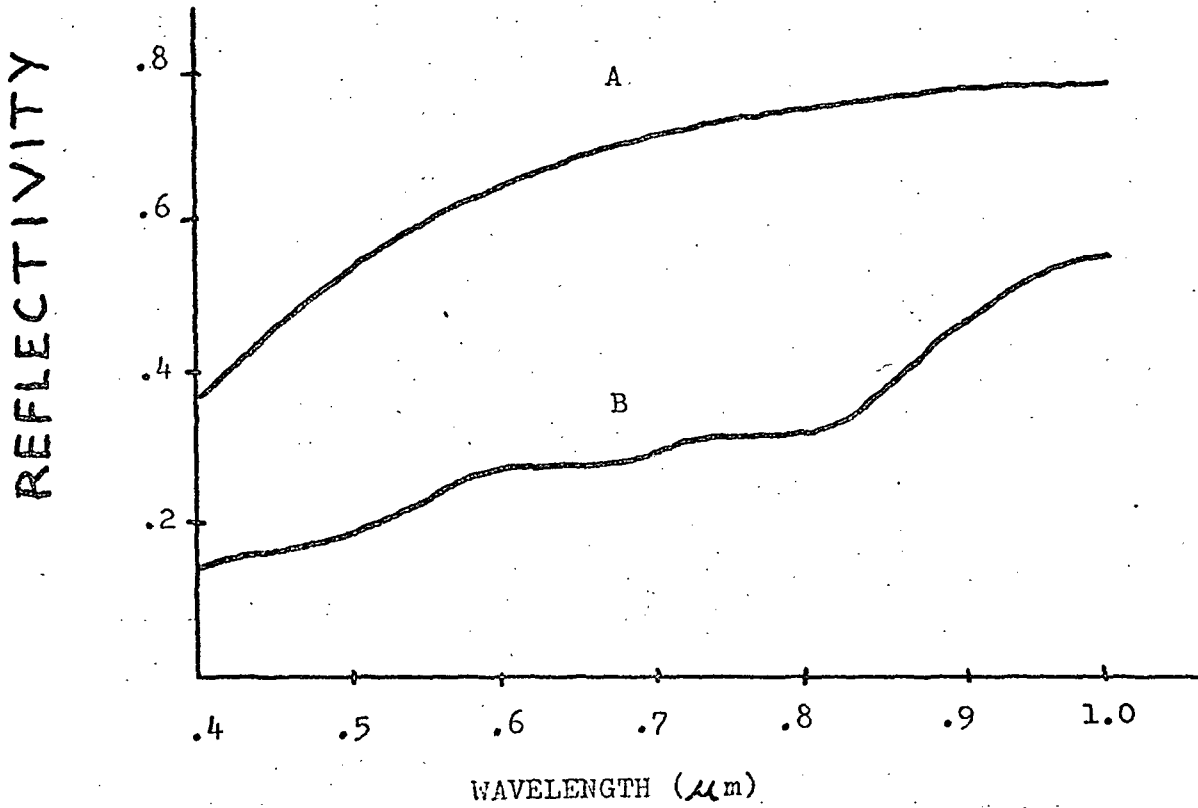
BIDIRECTIONAL REFLECTANCE RATIO

almost impossible to predict, an experiment is recommended for future work in this area. The primary objective of the experiment would be to determine the dynamic range of the reflectivity. Samples used in the experiment should be of varying degrees of roughness and material composition and measurements taken over a wide range of angles relative to the mean surface normal. The results of such an experiment could then be used to determine if controlled power output of the laser is necessary in order to prevent detector damage or detector saturation.

The spectral reflectance of two types of surfaces [8] is shown in Figure 10. The reflectance is assumed to be measured normal to the surface although the reference did not explicitly state how the measurement was made. In any case, it is important to note that the reflectivity increases as wavelength increases. The near infrared part of the spectrum is therefore a better choice than the visible part of the spectrum.

C. Detectors

Consideration must be given to the protection of the detector from intense radiation when the vehicle gets close to a specular surface. Under such conditions, almost the entire output of the laser could be focused upon the detector. As an example, consider a typical PbS detector [9] whose damage threshold is 0.32 J/cm^2 . A fast rise time detector [10] has an active area of approximately $2(10)^{-5} \text{ cm}^2$. Thus, the maximum input energy per pulse is $(0.32)(2)(10)^{-5} = 6.4(10)^{-6}$ Joules. If we consider a laser with a pulse width of 50 nsec., the damage threshold in terms of peak output power of the laser would be $6.4(10)^{-6}/50(10)^{-9} = 130$ watts. If the laser's output is restricted to be less than 130 watts peak, no damage will occur for this particular detector. Similar calculations



A. Limestone, Clay, Bright Objects
B Sands, Bare Areas in the Desert

Figure 10
SPECTRAL REFLECTANCE

could be made to determine the damage threshold in terms of peak power output of the laser for other detectors.

Another problem relating to excess radiation is saturation. The larger the input energy, the longer it will take for the detector to recover. This is due to the finite charge carrier lifetimes of semiconductor materials. Recovery time can be as long as several milliseconds^[9] which could restrict the maximum scan rate. In view of this, it is desirable to operate a detector with the lowest input that will produce a reasonable signal-to-noise ratio. This is also consistent with minimum laser powers.

Characteristics of several high speed photodiodes are given in Table III^[10]. It can be seen that there is a tradeoff between response time and peak efficiency. A diode with a response time of 0.13 nsec. has an efficiency of 40% whereas a similar diode with a response time of 7 nsec. has an efficiency of 90%. Note also that the slower diodes have larger sensitive areas. All of the photodiodes listed in Table III operate at room temperature (300° K).

D. Lasers

A semiconductor laser is probably the most likely candidate for use in the ranging system because of its small size and light weight. The spectral range of several semiconductor lasers is given in Table IV^[11]. Those shown in the table may be operated in pulsed mode at room temperature. A variety of GaAs lasers are commercially available^[12] with an energy conversion efficiency of about 4%. The nominal wavelength is 9050 Å with a drift rate of 2.5 Å/°C. The duty cycle of these devices is 0.1% for units with a peak power output of 10 watts or less. For output powers

Diode	Wavelength Range (μm)	Peak Efficiency (%)	Sensitive Area (cm^2)	Capacitance (pF)	Series Resistance (Ω)	Response Time (sec)	Dark Current (A)
Silicon $n^+ - p$	0.4-1	40	2×10^{-5}	0.8	6	1.3×10^{-10}	5×10^{-11}
Silicon p-i-n	0.6328	90	2×10^{-5}	1	1	1×10^{-10}	10^{-9}
Silicon p-i-n	0.4-1.2	90 @ 0.9 μm	5×10^{-2}	3	1	7×10^{-9}	2×10^{-7}
Ge $n^+ - p$	0.4-1.55	50	2×10^{-5}	0.8	10	1.2×10^{-11}	2×10^{-8}

TABLE III PHOTODIODE CHARACTERISTICS

Semiconductor Material	Wavelength (μm)
$\text{Al}_{1-x}\text{Ga}_x\text{As}$.63 - .90
$\text{GaAs}_{1-x}\text{P}_x$.61 - .90
GaAs	.83 - .91

TABLE IV WAVELENGTH OF SEVERAL
SEMICONDUCTOR LASERS

up to 300 watts, the duty cycle is 0.02%. If we assume a 50 nsec. pulse, the repetition rate for the low power devices is 20,000 pulses per second and for the high power devices is 4000 pulses per second. Thus, 1000 range measurements per second is a conservative estimate of the capability of the laser. Since the wavelength of the laser shifts with temperature, the spectral filter at the detector must be broad enough to accommodate this shift. A spectral filter with an optical bandwidth of 100 Å can tolerate a 40° C temperature shift. Consideration should be given to minimizing the temperature rise of the GaAs laser (i. e. by heat sinking) since the power output may decrease and a wider spectral filter will be required thus degrading the signal-to-noise performance of the system.

E. Electronic Scanners

An electronic scanning system is thought to be more desirable than a mechanical scanning system from the standpoint of reliability, weight and power. There is a wide range of electronically controlled scanners presently available [5]. These include piezo-electric devices, bender bimorphs, bimetallic strips, and electro-optic crystals. Of these, the piezo-electric laminated bimorph looks very promising. Power requirements are very small (milliwatts) and units with scan rates of 0.2 msec. with a 6° angular scan are commercially available. [13] Acousto-optic deflectors using lead-molybdate [14] can achieve scan rates of 300 kHz, but the angular scan is reduced to 2.5 milliradians. The total angular scan can be increased by using a lense, however the angular resolution will remain equal to that of the scanning device. Resolution varies, typically 100 to 400 elements. A two dimensional scan

can be achieved by using two scanning devices placed so that one scans perpendicular to the other. A possible scanning system is illustrated in Figure 11. An advantage of this configuration is that the transmitter and receiver use the same beam steering devices, thereby providing automatic tracking of the receiver.

IV CONCLUSION

The feasibility of using a laser to make range measurements from on board the Martian roving vehicle has been demonstrated. The weight and power requirements of a laser rangefinding system for use in a passive satellite navigation scheme have been estimated. The range error of such a system was explored in detail and was found to be within acceptable limits. The weight of the rangefinder was found to be a function of the transmitter beam divergence. In general, a smaller beam divergence resulted in less weight. Decreasing the beam divergence, however, increased the accuracy requirements of the pointing system used to search for the satellite. Some tradeoff between the weight of the laser and the weight of the pointing system will have to be made in a final design.

The feasibility of a laser rangefinder for mid-range path selection and obstacle avoidance has also been established. The range error for this system was explored in detail and was found to be acceptable. A surface reflectivity model has been presented for use in the final design of the system. Automatic gain control at the receiver and control of the laser output power may be necessary to overcome large changes in surface reflectivity. Electronic scanning of the laser beam was also investigated and found to be feasible.

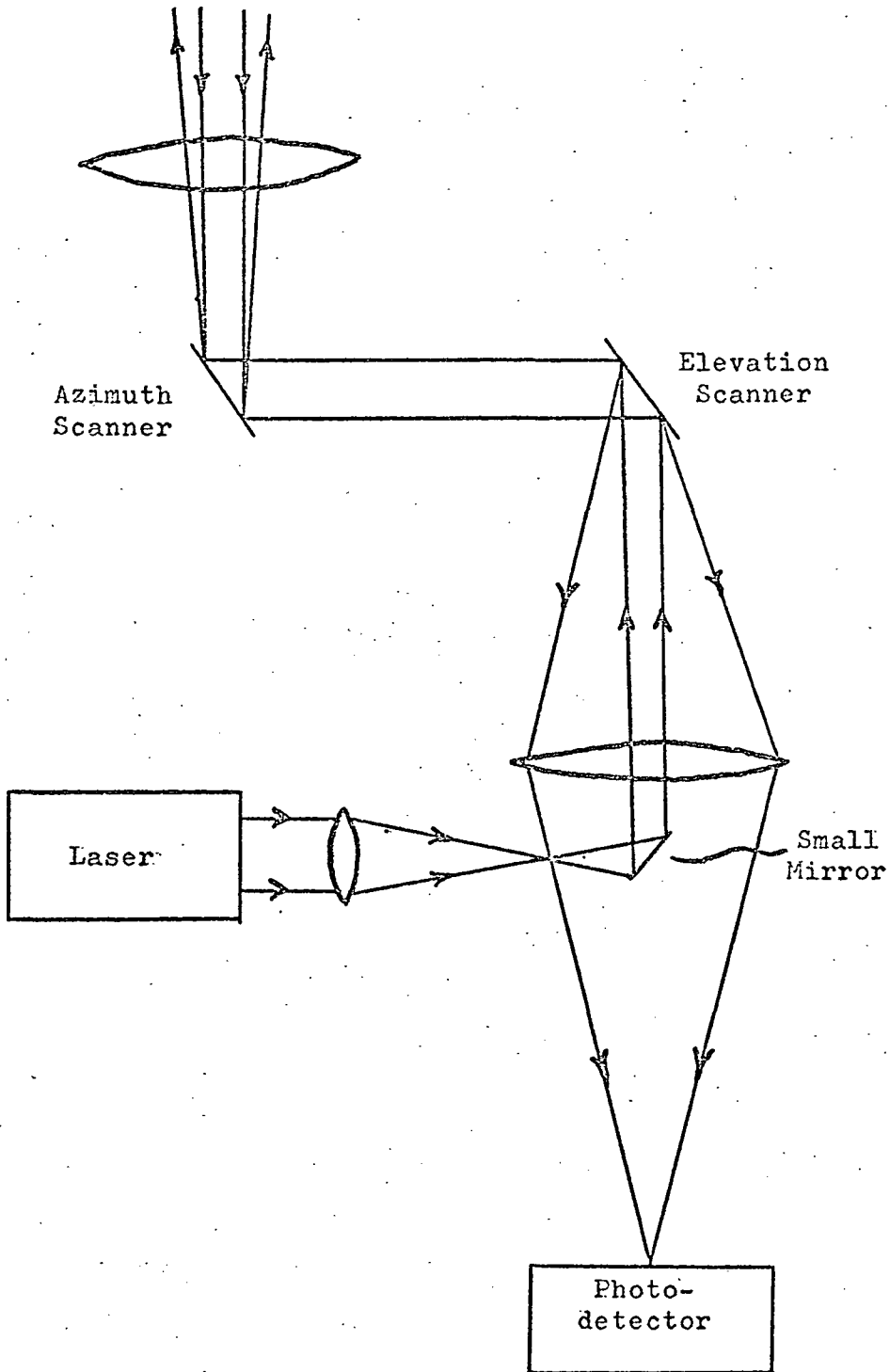


Figure 11

SCANNING SYSTEM

REFERENCES

1. Janosko, R. E., and Shen, C. N., "A Simplified Satellite Navigation System for an Autonomous Roving Craft", Rensselaer Polytechnic Institute, Troy, New York, 1972.
2. Carpentier, M. H., Radars: New Concepts, Gordon and Breach Science Publishers, 1968, pp. 68-71, 75-78.
3. Quelle, F. W., Jr., "Alternatives To Q-Spoiled Ruby Rangefinders", Proceedings SPIE, Laser Range Instrumentation Seminar, El Paso, Texas, Oct., 1967.
4. Ditchburn, R. W., Light, Interscience Publishers Inc., New York, 1953, p. 59.
5. Ross, Monte, Laser Applications, Academic Press, New York, 1971, pp. 282-283.
6. Advertisement by Maxwell Laboratories, Inc., Laser Focus, January, 1970, p. 18.
7. Torrance, K. E., Sparrow, E. M., "Theory for Off-Specular Reflection from Roughened Surfaces", Journal of the Optical Society of America, Vol. 57, No. 9, Sept., 1967, pp. 1105-1114.
8. Koechner, Walter, "Optical Ranging System Employing a High Power Injection Laser Diode", IEEE Transactions on Aerospace and Electronic Systems, Vol. AES-4, No. 1, Jan., 1968, pp. 81-91.
9. Stroller, Millan D., "Vulnerability of Lead Sulfide Detectors to Laser Radiation", Ballistic Research Labs, Aberdeen Proving Ground, MD., June, 1971.
10. Melchoir, Hans, et. al., "Photodetectors for Optical Communication Systems", Proceedings of the IEEE, Vol. 58, No. 10, Oct., 1970, pp. 1466-1483.
11. Geusic, et. al., "Coherent Optical Sources", Proceedings of the IEEE, Vol. 58, No. 10, Oct., 1970, p. 1429.
12. RCA Publication #OPT-100, "Gallium Arsenide Lasers and Emitters", 1970.
13. Advertisement by Coherent Optics Inc., Laser Focus, Feb., 1970, p. 13.
14. Advertisement by Orlando Research Corp., Laser Focus, March, 1970, p. 53.